

Classification of ADHD Patients by Kernel Hierarchical Extreme Learning Machine

Sartaj Ahmed Salman^{1,2}, Zhi Chao Lian², Yuduo Zhang²

¹Department of Informatics, The University of Electro-Communications, Chofu-Tokyo, Japan.

²School of Computer Science and Engineering, Nanjing University of Science and Technology, Nanjing, China.
s2140019@edu.cc.uec.ac.jp

Abstract. These days, the diagnosis of neuropsychiatric diseases through brain imaging technology has received more and more attention. The exploration of interactions in brain functional connectivity based on functional magnetic resonance imaging (fMRI) data is critical for the study of mental illness. Because attention-deficit/hyperactivity disorder (ADHD) is a chronic disease that affects millions of children, it is difficult to diagnose, so there is still much space for improvement in the accuracy of the diagnosis of the disease. In this paper, we consider the dynamics of brain functional connectivity, modeling a functional brain dynamics model from medical imaging, which helps to find differences in brain function interactions between normal control (NC) children and ADHD children. In more detail, our method is used by Bayesian Connectivity Change Point Model for dynamic detection, Local Binary Encoding Method for local feature extraction, and Kernel Hierarchical Extreme Learning Machine implementation classification. To validate our approach, experimental comparisons of fMRI imaging data on 23 ADHD and 45 NC children were performed, and our experimental methods achieved better classification results than existing methods.

Keywords. fMRI, BCCPM, local features, hierarchical extreme learning machine, ADHD, sparse-auto encoder

1. INTRODUCTION

The brain is the essential organ to command and correlate the actions and reactions of the human body, it is essential because it permits us to think, feel, and perform all the things that make us benevolent. These day's research on brain diseases is attaining courtesy and it's becoming a challenge for the researchers to make sure they are involved. In order to make sure that brain science is attaining courtesy, some niceties that are provided in this work. A neuropsychiatric disease Attention deficit hyper-activity disorder (ADHD) which is now considered as a common disease related to the brain, it's symptoms include the lack of attention, lack of activeness/hyperactive, and difficult to know some one's behavior [1]. Almost 3.4 % of children's all over the world are suffering from this disease [2]. It's difficult to diagnose because it doesn't have any physical symptoms, ADHD is an emergent disease like lack of knowledge. So, to find the difference between the children having ADHD and the children who don't these days a hot topic for the researchers. According to medical science, there are three types of this mental disorder which are given as Attention deficit hyper-activity disorder combined, Attention deficit hyper-activity disorder

hyperactive/impulsive, and Attention-deficit hyper-activity disorder in-attentive.

In the past physicians, doctors, or specialists/psychologists gather information from different sources such as ADHD checklists [3]. Now the Neuro Bureau provides preprocessed data to help the researchers to get more accurate results regarding this disease (nitrc.org) Different studies show that there are a lot of diseases which alters the functional connectivity of the brain, ADHD is also one of these kinds of disease [4]. The human brain is the most complex amongst all the other parts of a body. While coordinating with the body, the brain regions continuously change its formation and the regions generate temporary correlation are assumed to be connected functionally [5]. Brain function connection modeling can better understand the pathological basis of neurological disorders. Building a network of brain function connections can describe the interactions between various functions of the brain. For instance, a computational model is presented by Ou J et al. to characterize the AFIPs [6], this model has been extensively applied in the diagnosis of neurological disorders and the classification of different subtypes. In this paper, we apply the BCCPM [7] to find the time of dynamic change of brain function interaction. It will be described in detail in Section 2.1.

A lot of work has been reported on automatic diagnosis methods in the literature for extracting mass features from fMRI. In [8], Waqas Majeed et al. uses a new approach to observe that the reproducible spatiotemporal pattern of BOLD fluctuations is consistent with previous research and may have important information about brain activity at rest. This indicates that in the resting state, the brain is active. Many researchers have studied the dynamics of brain function connections. In [9], Lindquist M A, Waugh C, et al. uses the modified EWMA method to make it suitable for FMRI data, and then used it to analyze the change point of time series. In [10], Chang C et al. identified the dynamic connectivity of the brain with a sliding-window method. In [11], Ren, S., et al., recommend dynamic graph metrics to characterize temporal changes of functional brain networks. In [5], Atif Riaz Muhammad Asad Eduardo uses a Hybrid framework that employs affinity propagation clustering and density peak for functional connectivity. During the past few years, many researchers introduced different types of models for the classification of ADHD.

Medically, brain disorders have been diagnosed primarily by subjective observation. Many studies have identified it as a two-category problem, such as ADHD and non-ADHD. In [12], Gülay Çiçek et al. created two separate datasets, gray level co-occurrence matrix dataset and Haralick texture features dataset and uses machine learning algorithms to classify. In [13], Miao Bo and Y. Zhang uses the feature extraction method based on Relief and VA-Relief to achieve high-precision classification. In [14], Sudha, D., and M. P. Rani extracted the gait signal characteristics of ADHD children in the video to study disease diagnosis and strengthen the cognition of sick children. In [15], Chang et al use a feature extraction method based on a texture point of view using the isotropic local binary patterns on three orthogonal planes (LBP-TOP) and design support vector machine (SVM) model to classify. In [16], Athena Taymourtash, Farnaz Ghassemi use sparse based representation method by extracting the feature by cluster ICs and uses k-nn classifier to find out the EEG source differences between adults with ADHD and healthy controls. In [17], Yan Zhang et al. introduced classification by using feature space separation with sparse representation and proposed classification framework with the dual diagnosis model based on sparse. In [18], Juan L. Lopez Marcano et al. explained that the United States allows using the θ/β power ratio (TBPR) as a diagnostic feature of ADHD. In [19], F.M. Grisales-Franco et al. uses a Dynamic Sparse Coding (DSC) method based on physiologically motivated Spatio-temporal constraints to construct non-stationary brain activity, they search the difference between ADHD and control groups using statistical results.

To design a computational model with high precision to classify ADHD is quite challenging. So, we proposed a novel classification framework for the diagnosis of ADHD in this paper, which is a new contribution to classify children having ADHD and the children who don't. The novel classification framework proposed consists of three parts (see Fig. 1). In the first part, dynamic detection is performed by BCCPM because the brain functional connections are dynamic. In the second part, LBEM extracts the characteristics of the brain in each sample. The last part uses several classifiers to classify brain data to distinguish between ADHD patients and NC. In order to verify the necessity of dynamic detection of the brain and the accuracy of the classifier. We have experimented with different classification methods on the sample sets that have undergone dynamic detection and no dynamic detection, indicating that our newly proposed classification framework has more accurate classification results for the diagnosis of ADHD patients.

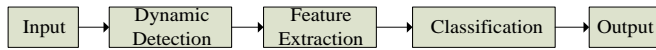


Fig. 1. The data processing flow chart of the classification framework proposed in our paper.

2. Proposed Algorithms

2.1 Bayesian Connectivity Change Point Model (BCCPM)

The BCCPM is used as a dynamic detection for the brain. Previous studies have shown that the brain has a series of

dynamic changes even in the resting state, which affects the interaction of brain function connections. If the data is classified directly without dynamic detection, the performance is not satisfied. Therefore, we refer to the method [7] to dynamically divide the time period into several time blocks, that is, to find the time point of the brain dynamic change activity. Next, we will briefly introduce BCCPM.

With BCCPM, the data matrix $Z = (z_1, z_2, \dots, z_T)$ can be divided into several time blocks. The matrix Z consists of T m-dimensional vectors, each vector representing the value of m ROIs (Regions of Interest) at time t . Where each vector in Z satisfies the independent and identical distribution, and $z_t \sim N(\mu, \Sigma) t = 1, 2, \dots, T$.

Here an indication vector $\vec{L} = (L_1, L_2, \dots, L_T)$ is used, where $L_t = 1$ represents the change point and specifies $L_1 = 1$, $L_t = 0$ means unchanged. Then the likelihood of Z is as follows:

$$p(Z|\vec{L}) = \prod_{b=1}^{\sum L_i} p(Z_b) \quad (1)$$

where $\sum L_i$ is the number of time blocks divided, and $p(Z_b)$ can be obtained by the following equation (2) [20]:

$$p(z_1, z_2, \dots, z_T) = \frac{p(z_1, z_2, \dots, z_T; \mu, \Sigma)}{p(\mu, \Sigma|z_1, z_2, \dots, z_T)} = \frac{(\frac{1}{2\pi})^{mT/2} \left(\frac{k_0}{k_T}\right)^{m/2} \Gamma_m\left(\frac{v_T}{2}\right) (\det(\Lambda_0))^{v_0/2}}{\Gamma_m\left(\frac{v_0}{2}\right) (\det(\Lambda_T))^{v_T/2}} 2^{mT/2} \quad (2)$$

where Γ_m is the multivariate gamma function.

Since Z is divided into independent time blocks from each other, the posterior distribution of $p(\vec{L}|Z)$ is as follows:

$$p(\vec{L}|Z) \propto p(\vec{L}) \cdot p(Z|\vec{L}) \quad (3)$$

and $p(\vec{L}) = \sum_{t=1}^T p(L_t)$, where $p(L_t) \sim \text{Bern}(0.5)$. Finally, we use the Markov-chain Monte-Carlo [21] with random \vec{L} , to generate samples with the posterior distribution $p(\vec{L}|Z)$. Refer to [7] for details.

2.2 Local Binary Encoding Method (LBEM)

In order to extract the local information of the brain function interaction patterns (FIPs), our previous research proposed that LBEM [22] can be applied to the local feature extraction of fMRI data.

LBEM is used to process the data object DICCOL-fMRI. DICCOL-fMRI is the dataset matrix $D = (D_1, D_2, \dots, D_T) \in \mathbb{R}^{358 \times T}$, each vector $D_t = (d_1, d_2, \dots, d_{358})$, $1 \leq t \leq T$ representing the value of 358 ROIs at time t .

First, recode each column vector D_t in data matrix D . Comparing each element in D_t with its neighboring elements yields a new vector $F_t = (f_1, f_2, \dots, f_{714})$, $1 < t < T$ is calculated by the equations (4-6):

$$f_{2(i-1)-1} = \begin{cases} 1, & d_i \leq d_{i-1}, 2 \leq i \leq 358 \\ 0, & d_i > d_{i-1} \end{cases} \quad (4)$$

$$f_{2(i-1)} = \begin{cases} 1, & d_i \leq d_{i+1}, 2 \leq i \leq 357 \\ 0, & d_i > d_{i+1} \end{cases} \quad (5)$$

$$f_{714} = \begin{cases} 1, & d_{358} \leq d_1 \\ 0, & d_{358} > d_1 \end{cases} \quad (6)$$

Then we get a matrix of binary form containing only 0 and 1 elements $F = (F_1, F_2, \dots, F_T) \in R^{714 \times T}$. Figure 2 depicts an example of a binary form conversion. As shown, the vector $A = (a_1, a_2, a_3, a_4)$ is encoded to obtain the vector $B = (b_1, b_2, \dots, b_6)$. Since $a_2 < a_1$ assigns b_1 to 1, and $a_2 > a_3$ assigns b_2 to 0. The values of b_3, b_4, b_5 can be obtained in the same way. The final assignment b_6 is equal to 1, because of $a_4 < a_1$.

Second, we convert each binary form of vector in F to a decimal form. Each of the six elements in the vector F_t is divided into a group. Then, each group number is converted from a 6-bit binary form to a decimal form, and the range of the converted decimal number is $[0, 63]$. After F is transformed, we get the data matrix $E = (E_1, E_2, \dots, E_T) \in R^{119 \times T}$ which represents the local information between each ROI and its adjacent ROIs. The example is shown in Fig. 2.

Third, we will perform histogram equalization processing for each row vector of the data matrix E obtained in the second

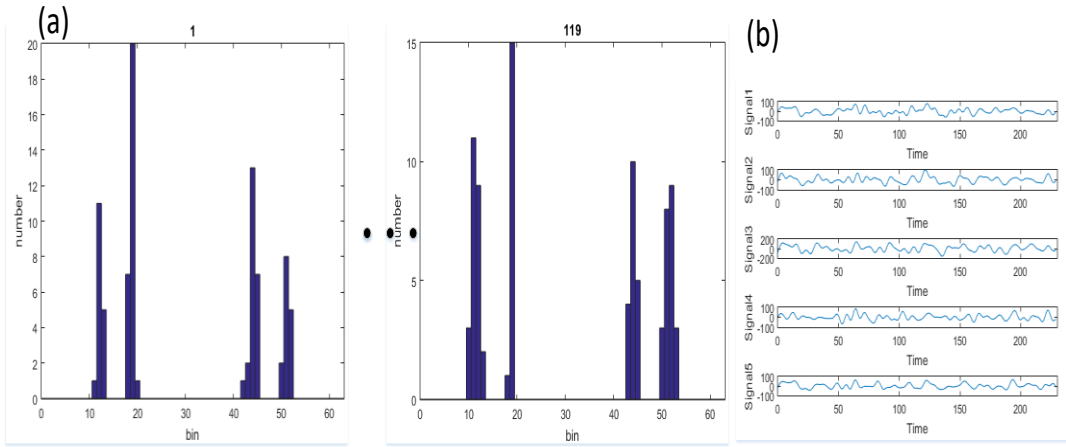


Fig. 3. (a) After histogram equalization, 119 histograms were obtained. (b) The r-fMRI signal of five DICCCOLs in one sample.

2.3 Classification Via KELM Algorithm

For a better understanding of KELM [23], let's briefly review the ELM [24] theory. The ELM only has one hidden layer H containing L hidden nodes. For the G classification problem, given a training set $\{(x_j, z_j) | x_j \in R^d, z_j \in R^G\}$, where x_j is the training vector, z_j is the training label, and $j = 1, 2, \dots, N$. The ELM algorithm can be described as follow:

1. Calculate the hidden layer matrix H

$$H = \begin{bmatrix} h(x_1) \\ \vdots \\ h(x_N) \end{bmatrix} \begin{bmatrix} h(w_1 x_1 + b_1) & \dots & h(w_L x_1 + b_L) \\ \vdots & \ddots & \vdots \\ h(w_1 x_N + b_1) & \dots & h(w_L x_N + b_L) \end{bmatrix} \quad (7)$$

where $h(\cdot)$ denotes the nonlinear activation function, the input weights w_i and biases b_i are randomly generated, $i=1, 2, \dots, L$.

2. The output weight vector β can be calculate by equation (8).

$$\beta = H^\dagger Z \quad (8)$$

where H^\dagger is the Moore-Penrose generalized inverse of matrix H , and Z is the training label matrix

$$Z = \begin{bmatrix} Z_1^T \\ \vdots \\ Z_N^T \end{bmatrix} = \begin{bmatrix} Z_{11} & \dots & Z_{1G} \\ \vdots & \ddots & \vdots \\ Z_{N1} & \dots & Z_{NG} \end{bmatrix} \quad (9)$$

The corresponding result of ELM can be obtained as follow:

$$f(x_j) = h(x_j)\beta \quad (10)$$

In KELM, a kernel matrix $\Omega_{\text{ELM}} = HH^T: \Omega_{\text{ELM}} = h(x_p) \cdot h(x_q) = K(x_p, x_q)$ is applied. Then, the kernel case of ELM output function is:

$$f(x_j) = \begin{bmatrix} K(x_j, x_1) \\ \vdots \\ K(x_j, x_N) \end{bmatrix}^T \left(\frac{1}{\rho} + \Omega_{\text{ELM}} \right)^{-1} Z \quad (11)$$

In this work, a radial basis function as Ω_{ELM} is used to achieve better experimental results.

2.4 Classification Via KH-ELM Algorithm

The KH-ELM has more complex structure than KELM, the training algorithm in the KH-ELM is different from the greedy lay-wise [25]. The architecture of KH-ELM is shown in Fig. 4. It consists of two parts: 1) the unsupervised hierarchical feature extraction based on the ELM Sparse-auto encoder and 2) the supervised classification based on KELM.

For the G classification problem, given a training set $\{(x_j, z_j) | x_j \in R^d, z_j \in R^G\}$, where x_j is the training vector, z_j is the training label, and $j = 1, 2, \dots, N$. Before the unsupervised hierarchical feature extraction, the dataset should be simply scaled to $[0, 1]$ and the labels are resized to G dimension which are -1 or 1. Then the input data is mapped into the ELM random feature space and its extract through n-layer unsupervised learning feature. For KH-ELM learning algorithm, it takes the input layer as layer 0, the first layer is a hidden layer, the first layer weights β_1 is learned by the ELM Sparse-auto encoder which is shown in Fig. 4 (a), and other hidden layer weights are also learned by the ELM Sparse-auto encoder. The result of each hidden layer can be calculated by

$$H_i = g(H_{i-1} \cdot \beta^T), 1 \leq i \leq n \quad (12)$$

where H_i is the output of the i th layer, H_{i-1} is the output of the $(i-1)$ th layer, $g(\cdot)$ is the activation function of the hidden layers, and β is the i th hidden layer weight (output weight) [26]. For KH-ELM, each hidden layer is an independent module. Once the feature of the previous hidden layer is extracted, the weights of the current hidden layer will be fixed without fine-tuned [27]. Here the L1 norm is used regularization to build an ELM Auto encoder, so the resulting ELM Sparse-auto encoder gives better generalization performance to the parameters. In addition, the use of penalty term can constrain our model features. This allows the learned model to have sparser

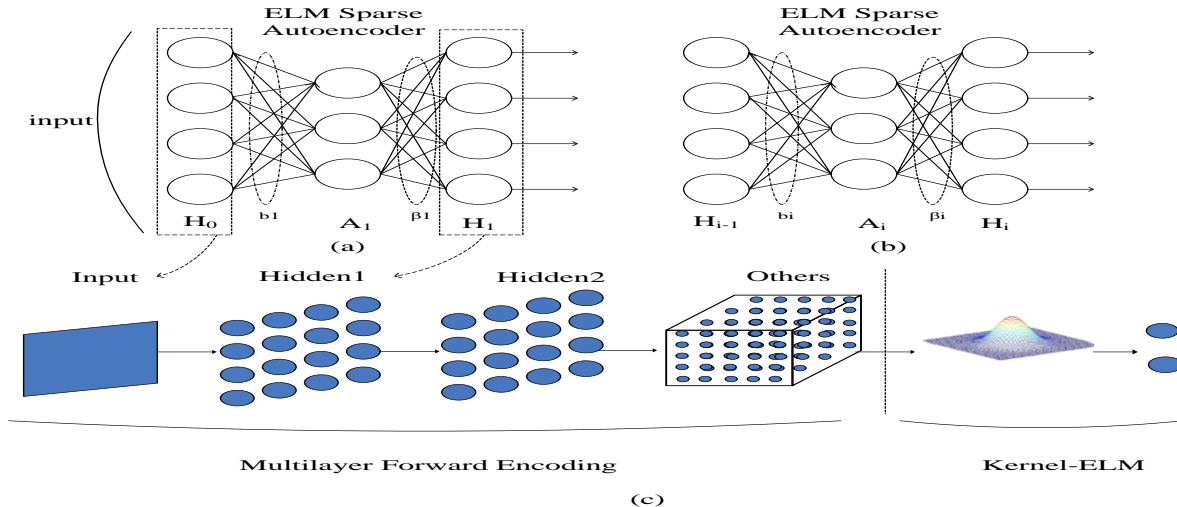


Fig. 4. (a)The ELM Sparse Autoencoder structure of the first hidden layer. (b)The ELM Sparse Autoencoder structure of the i th hidden layer. (c)The architecture of the KH-ELM learning algorithm [33]

characteristics. The ELM Sparse-auto encoder equation for this optimization model is expressed as follows:

$$O_\beta = \text{argmin}_\beta \{||A\beta - X||^2 + ||\beta||_{l1}\} \quad (13)$$

Where A denotes the random mapping output, β is the hidden layer weight to be obtained, X represents the input data. In the proposed auto encoder, A is a random initialized output mapped by a random weight matrix $b = [b_1, b_2, \dots, b_n]$, which does not require optimization. The structure of the ELM Sparse-auto encoder is shown in Fig 4 (a) (b). As shown, this not only saves training time but also improves learning accuracy.

Next the ELM optimization algorithm based on Sparse-auto encoder is described. The fast-iterative shrinkage-threshold algorithm (FISTA) is used to solve the constraint minimization problem of continuously differentiable functions. We use a constant-step type of FISTA. The specific algorithm is described as follows:

1. Calculate the Lipschitz constant γ of the gradient ∇p of the function $||A\beta - X||^2$

2. Calculate β iteratively. Begin the iteration by taking $y_1 = \beta_0 \in R^n$, $t_1=1$ as the initial points. Then, for i ($i \geq 1$)

Step 1. $\beta_i = S_\gamma(y_i)$, Where

$$S_\gamma = \text{arg min}_\beta \left\{ \frac{\gamma}{2} \|\beta - (\beta_{i-1} - \frac{1}{\gamma}(\beta_{i-1}))\|^2 + \|\beta\|_{l1} \right\}$$

$$\text{Step 2. } t_{i+1} = \frac{1 + \sqrt{1 + 4t_i^2}}{2}$$

$$\text{Step 3. } y_{i+1} = \beta_i + \left(\frac{t_{i-1}}{t_{i+1}} \right) (\beta_i - \beta_{i-1})$$

The second part of KH-ELM is the supervised feature classification based on KELM. The KELM input is matrix H_n that is the output of n-layer ELM Sparse Autoencoder.

3. Experimental Results and Analysis

In this section, in order to prove that our proposed ADHD classification framework has a more accurate and stable classification effect, we conducted a comparative experiment on the r-fMRI dataset [6] containing 23 ADHD patients and 45 NC. We first select 358 landmarks [28] as nodes of the network. The DICCOL was determined for 68 subjects using a commonly available tool in [29], and the r-fMRI signal corresponding to each DICCOL was extracted. As shown in Fig. 3 (b), the r-fMRI signal of five DICCOLs in one sample is represented. After preprocessing, we get a 358*270-time series matrix for each sample in the dataset. Then the r-fMRI time series of each sample was dynamically detected by BCCPM to obtain a time series matrix of 358*230.

In this work, the 5-fold cross-validation method is used to appraise the proposed method. The experiment was repeated 30 times and then calculated the average classification accuracy of each fold. For the purpose of comparing the accuracy of classification under different methods, we compared the experimental results of three different classification methods of KH-ELM, KELM and Jinli Ou's method [6], the experimental results of KELM with different kernels and the experimental results of KH-ELM with different layers were compared. Firstly, it is showed that our method with KELM achieved better performance (average accuracy of ADHD is 95.51% and NC is 97.57%), compared to the results of Ou's [6] (average accuracy of ADHD is 92% and NC is 95%). In addition, comparing Jinli Ou's method, KELM obtained more stable classification results, the comparison results show that it is effective to extract local features using LBEM. Then, it shows that KH-ELM's classification accuracy results which are shown in the first column of Table I (97.17% for the ADHD and 99.76% for the NC) is higher than that of KELM, shows that using the ELM sparse-auto encoder to extract features from the training dataset and the test dataset before the KELM improve the classification accuracy.

To verify the necessity of dynamic detection under r-fMRI data for each subject after pretreatment. We conducted a controlled experiment on data processed by BCCPM and data processed without BCCPM. Both sets of experiments used a five-fold cross-validation method, using LBEM to extract local features and then classifying them with KELM. We repeated the experiment 30 times and recorded the average classification result for each fold. The experimental results are shown in Table 1. respectively. The results show that after the dynamic detection, using same classification method gets better classification accuracy, and proves that the brain has time dynamics even in the resting state.

Finally, we compare the effect of different parameters on the classification accuracy. We analyze the results by two types of parameters a) we repeated the whole experiment with RBF kernel and linear kernel. While using two different kernel functions, RBF kernel function has higher precision the experimental results are shown in Table 2. It can be seen that in addition to linear kernel function kernel (average ADHD is 60.55%, average precision of NC is 96.06%), the calculation result of RBF kernel (average precision of ADHD is 96.92%, average precision of NC is 99.2%) function is more accurate.

Here, we get better results with RBF kernel, which has been demonstrated by different researchers comparing different kinds of work with different kernels [30,31]. b) the effect of increasing number of hidden layers on the classification accuracy using KH-ELM. Same method was used for HELM to make a comparative experiment, and the results are shown in Table 3. (59.19% for ADHD and 85.97% for NC). Experiments show that the classification results of HELM [32] are very unstable compared to the high classification accuracy of KH-ELM. For the effect of increasing number of hidden layers on the classification accuracy, Table 3. shows the experimental results using KH-ELM with three hidden layers (41.80% for ADHD and 66.67% for NC) and with one hidden layer (97.17% for ADHD and 99.76% for NC).

We found that with the increasing number of hidden layers, the accuracy of classification results is lower. To explain this more clearly we performed the same operation up-to six hidden layers. Our experiment is the same as the previous one, repeat experiment 30 times, recording the average result of each folding, increasing the number of layers one by one. The experimental results are shown in Table 4 and 5. These days most of the deep learning methods show that it will get better result with increasing number of hidden layers, but in our experiments we got worse results with the increasing number of layers. The reason we came to this conclusion, when we conduct multi-layer experiments after each layer, it will extract some features and lead to the repetition of features, and at the same time, more features will be produced. These features are inconsistent with the algorithm proposed and will have the greatest impact on the results as the number of layers increases as the extension layer is limited. After that, we no longer extract features, but tend to "over-fit" data and over-fitting will reduce the accuracy of the experiment. Therefore, KH-ELM classification with only one hidden layer to extract feature is better than the multi-hidden layer feature.

4. Conclusion

In this paper, we propose a novel classification scheme to improve the accuracy of brain data classification for distinguishing between ADHD patients and NC. The innovation of our paper is the use of hierarchical ELM sparse autoencoder to extract feature before KELM which outperformed other classifiers that have been used to distinguish between ADHD patients and NC, while requiring fewer hidden layers. The comparison of experimental results at different scales shows that the classification accuracy with dynamic detection is higher, and the selection of the number of layers for classifier feature extraction is not as good as possible. As the future work, we hope to have more experiments to improve the average accuracy of fMRI classification for distinguishing between ADHD patients and NC.

Acknowledgment

The authors would like to thank Prof. Tianming Liu and his group CAID for providing the ADHD data. This work was supported by the Major Research plan of the National Natural Science Foundation of China (No. 91538108), the National Natural Science Foundation of China (No. 61501241,61571230), the Natural Science Foundation of Jiangsu Province (No. BK20150784,BK20150792,

BK20161500), and the China Postdoctoral Science Foundation (No. 2015M570450, 2015M581800).

Table 1. Average accuracy comparison using different methods

Class	Proposed Method KH-ELM		Method KELM		Method KELM Without BCCPM		Jinli Ou's Method	
	NC	ADHD	NC	ADHD	NC	ADHD	NC	ADHD
Fold1	0.9973	1	0.9747	0.9522	0.7111	0.44	0.8889	1
Fold2	0.9907	1	0.9779	0.9449	0.7778	0.4	0.8889	0.8
Fold3	1	0.9974	0.983	0.959	0.6222	0.4	1	0.8
Fold4	1	0.9564	0.9711	0.9463	0.6667	0.55	1	1
Fold5	1	0.9048	0.972	0.9731	0.5556	0.3	1	1
Average	99.76%	97.17%	97.57%	95.51%	66.67%	41.80%	95.00%	92.00%

Table 2. Average accuracy comparison using different kernels

Class	Proposed Method Using RBF kernel		Proposed Method Using Linear kernel	
	NC	ADHD	NC	ADHD
Fold1	1	0.8462	0.9615	0.6154
Fold2	0.9600	1	0.9600	0.6154
Fold3	1	1	0.9600	0.6429
Fold4	1	1	0.9615	0.6923
Fold5	1	1	0.9600	0.4615
Average	99.2%	96.924%	96.06%	60.55%

Table 3. The comparison of classification accuracy in different parameters

Class	Proposed Method KH-ELM with Three Hidden Layer		Proposed Method KH-ELM with One Hidden Layer		Proposed Method HELM	
	NC	ADHD	NC	ADHD	NC	ADHD
Fold1	0.7111	0.44	0.9973	1	0.8667	0.5974
Fold2	0.7778	0.4	0.9907	1	0.892	0.4692
Fold3	0.6222	0.4	1	0.9974	0.8267	0.6359
Fold4	0.6667	0.55	1	0.9564	0.8667	0.6
Fold5	0.5556	0.3	1	0.9048	0.8462	0.6571
Average	66.67%	41.80%	99.76%	97.17%	85.97%	59.19%

Table 4. The comparison of classification accuracy in different parameters

Class	Proposed Method KH- ELM with One Hidden Layer		Proposed Method KH- ELM with second Hidden Layer		Proposed Method KH-ELM with Third Hidden Layer	
	NC	ADHD	NC	ADHD	NC	ADHD
Fold1	0.9973	1	0.9423	0.9025	0.7111	0.44

Fold2	0.9907	1	0.972	0.7974	0.7778	0.4
Fold3	1	0.9974	0.976	0.9642	0.6222	0.4
Fold4	1	0.9564	0.9667	0.9359	0.6667	0.55
Fold5	1	0.9048	0.9586	0.8846	0.5556	0.3
Average	99.76%	97.17%	96.31%	89.69%	66.67%	41.80%

Table 5. The comparison of classification accuracy in different parameters

Class	Proposed Method KH-ELM with Forth Hidden Layer		Proposed Method KH-ELM with Fifth Hidden Layer		Proposed Method KH-ELM with Sixth Hidden Layer	
	NC	ADHD	NC	ADHD	NC	ADHD
Fold1	0.8307	0.3538	0.7474	0.3743	0.7397	0.3512
Fold2	0.7693	0.5230	0.688	0.5025	0.6973	0.5051
Fold3	0.7213	0.6278	0.7026	0.5380	0.7346	0.5166
Fold4	0.8359	0.5256	0.7538	0.4461	0.7667	0.4410
Fold5	0.724	0.5820	0.672	0.5615	0.644	0.4897
Average	77.62%	52.24%	71.27%	48.45%	71.64%	46.07%

References

- [1] I. Singh, "Beyond polemics: Science and ethics of ADHD," *Nature Rev. Neurosci.*, vol. 9, no. 12, pp. 957–964, Dec. 2008.
- [2] G. V. Polanczyk, G. A. Salum, L. S. Sugaya, A. Caye, and L. A. Rohde, "Annual research review: A meta-analysis of the worldwide prevalence of mental disorders in children and adolescents," *J. Child Psychol. Psychiatry*, vol. 56, no. 3, pp. 345–365, Feb. 2015.
- [3] Barkley, R.A.: Attention-Deficit Hyperactivity Disorder: A Handbook for Diagnosis and Treatment, 3rd edn. The Guilford Press, New York (2005)
- [4] Van Den Heuvel, M.P., Pol, H.E.H., 2010. Exploring the brain network: a review on resting-state fMRI functional connectivity. *Eur. Neuro psychopharmacology*. 20 (8), 519–534.
- [5] Atif Riaz*: Fusion of fMRI and non-imaging data for ADHD classification: Computerized Medical Imaging and Graphics 65 (2018) 115–128, 16 October 2017 0895-6111/ © 2017 Elsevier
- [6] J. Ou, Z. Lian, et al., "Atomic dynamic functional interaction patterns for characterization of ADHD," *Human Brain Mapping*, vol. 35, no. 10, pp. 5262–5278, 2014.
- [7] Lian, Zhi chao, et al. "Exploring functional brain dynamics via a Bayesian connectivity change point model." 2014 IEEE 11th International Symposium on Biomedical Imaging (ISBI 2014) IEEE, 2014.
- [8] W. Majeed, M. Magnuson, et al., "Spatiotemporal dynamics of low frequency BOLD fluctuations in rats and humans," *Neuro Image*, vol. 54, pp. 1140–1150, 2011.
- [9] Lindquist, Martin A, C. Waugh, and T. D. Wager. "Modeling state-related fMRI activity using change-point theory." *Neuro image* 35.3(2007):1125-1141.
- [10] Chang, Catie, and G. H. Glover. "Time – frequency dynamics of resting-state brain connectivity measured with fMRI." *Neuroimaging* 50.1(2010):81-98.
- [11] Ren, S., et al. "Dynamic Functional Segregation and Integration in Human Brain Network During Complex Tasks." *IEEE Transactions on Neural Systems & Rehabilitation Engineering* a Publication of the IEEE Engineering in Medicine & Biology Society 25.6(2016):547-556.
- [12] Gülay Çiçek, A. Akan, and Z. Orman. "Classification of ADHD by using textural analysis of MR images." *Medical Technologies National Congress* 2017:1-4.
- [13] Miao, Bo, and Y. Zhang. "A feature selection method for classification of ADHD." *International Conference on Information, Cybernetics and Computational Social Systems* 2017:21-25.
- [14] Sudha, D., and M. P. Rani. "Gait Classification for ADHD Children Using Modified Dual Tree Complex Wavelet Transform." *World Congress on Computing and Communication Technologies IEEE Computer Society*, 2017:215-218.
- [15] Che-Wei Chang, Chien-Chang Ho and Jyh-Horng Chen ADHD classification by a texture analysis of anatomical brain MRI data
- [16] Athena Taymourtash, Farnaz Ghassemi Independent Component analysis of sparse transformed EEG signal for ADHD/Normal Adult classification 978-1-4799-1972-7/15/\$31.00 c 2015 IEEE
- [17] Yan Zhang : ADHD classification by feature space separation with sparse representation: DSL 2018: 1-5
- [18] Marcano, Juan L. Lopez, M. A. Bell, and A. A. L. Beex. "Classification of ADHD and Non-ADHD using theta/beta

power ratio features." IEEE Embs International Conference on Biomedical & Health Informatics IEEE, 2017.

[19] F.M. Grisales-Franco, J.M. Medina-Salcedo, D.M. Ovalle-Martínez3, J.D. Martínez-Vargas1(B), D.G. Garcíá-Murillo1, and G. Castellanos-Dominguez1 EEG Source Imaging Based on Dynamic Sparse Coding as ADHD Biomarker IWINAC 2017, Part I, LNCS 10337.

[20] B. A. Gelman, J. B. Carlin, H. S. Stern, D. B. Rubin (2003): Bayesian Data Analysis, Second Edition, Chapman & Hall/CRC Texts in Statistical Science.

[21] J. Liu (2001): Monte Carlo Strategies in Scientific Computing. Springer. 2001.

[22] Li, Yang, et al. "ELM-based classification of ADHD patients using a novel local feature extraction method." IEEE International Conference on Bioinformatics & Biomedicine IEEE, 2017.

[23] G. B. Huang, "An Insight into Extreme Learning Machines: Random Neurons, Random Features and Kernels," Cognitive Computation, vol. 6, pp. 376-390, 2014.

[24] G.B. Huang, Q. Zhu, and C.K. Siew, "Extreme learning machine: theory and applications," Neuro computing, vol. 70, no.1, pp. 489-501, 2006.

[25] Duan, Lijuan, et al. "Motor Imagery EEG Classification Based on Kernel Hierarchical Extreme Learning Machine." Cognitive Computation9.6(2017):1-8.

[26] Y. Bengio, "Learning deep architectures for AI," Found. Trends Mach. Learn., vol. 2, no. 1, pp. 1-127, 2009.

[27] Bo Chen, Xiang Li. "Temporal functional connectomes in schizophrenia and healthy controls", 2017 IEEE International Conference on Systems, Man, and Cybernetics (SMC), 2017.

[28] Tang, J., C. Deng, and G. B. Huang. "Extreme Learning Machine for Multilayer Perceptron." IEEE Transactions on Neural Networks & Learning Systems 27.4(2017):809-821.

[29] Marcano, J. L., et al. "Classification of ADHD and non-ADHD using AR models. " International Conference of the IEEE Engineering in Medicine & Biology Society Conf Proc IEEE Eng Med Biol Soc, 2016:363

[30] Gatot Wahyudi, Muhammad Ivan Fanany, Wisnu Jatmiko, and Aniati Murni Arymurthy et al, "SVM Kernels Accuracy and Generalization Capability on Apnea Detection from ECG" ICACIS 2010.

[31] Deping Kuang, Lianghua He Classification on ADHD with Deep Learning 978-1-4799-6621-9 /14 \$31.00 © 2014 IEEE

[32] X. Zhang, L. Guo, X. Li, T. Zhang, et al., "Characterization of Task-free and Task-performance Brain States via Functional Connectome Patterns.,," Medical Image Analysis, vol. 17, pp. 1106–1122, 2013.

[33] Qureshi, M. N., et al. "Classification of ADHD subgroup with recursive feature elimination for structural brain MRI. " Engineering in Medicine and Biology Society IEEE, 2016:5929.